THE BELL SYSTEM TECHNICAL JOURNAL
Vol. 62, No. 5, May–June 1983
*Printed in U.S.A.*

# Modal Analysis of Loss and Mode Mixing in Multimode Parabolic Index Splices

By I. A. WHITE and S. C. METTLER

(Manuscript received November 18, 1982)

*In this paper we present an electromagnetic modal theory for characterizing parabolic-index multimode fiber splices with either intrinsic or extrinsic mismatches. The theory agrees with previously published theoretical results for transverse offset using a uniform power distribution. It also agrees with new experimental measurements made with a long, spliced input fiber using a published, theoretical, steady-state modal power distribution. This modal theory predicts, and experiment confirms, a previously unreported periodic fluctuation in splice loss as a function of wavelength for intrinsic parameter mismatch. The analysis also predicts a large degree of mode mixing for transverse offset but negligible mode mixing for parameter mismatch in typical multimode fiber splices.*

## I. INTRODUCTION

Theoretical predictions of splice loss in multimode fibers have been attempted by many researchers (see Ref. 1 for a list). However, these analyses[1–3] do not adequately predict measured splice loss results, and most do not address mode mixing effects, which are important for the prediction of the bandwidth of concatenated lengths of fiber. The best agreement with splice loss measurement data is an empirical model based on geometric optics.[2] However, such an analysis of splice loss provides only a limited description of the effect of splices. Electromagnetic theory, using the coupling coefficients of individual modes, provides a complete treatment of splice loss and mode mixing. The only published electromagnetic theory[3] appears to be in error, since predictions do not approach the well-known correct geometric optics limit for splice loss of fibers with a large normalized frequency, $V$, and a uniform modal power distribution. This paper presents an electromagnetic analysis for splices, which gives single-term expressions for mode

coupling coefficients for the case of either transverse offset or profile parameter mismatch for parabolic-index multimode fibers. These coupling coefficients are used to calculate loss and degree of mode mixing in splices. The results approach the proper geometric optics limit for a uniform modal power distribution. Furthermore, if we compare theoretical and experimental loss to transverse offset results, we can verify a published theoretical "steady-state" power distribution[4] in multimode parabolic-index fibers. Comparing the results of this theory with a measurement of splice loss as a function of transverse offset gives the modal power distribution in a fiber. A wavelength dependence of splice loss for intrinsic parameter mismatch is predicted by this theory and has been experimentally verified. Because splices change the modal power distribution, the power redistribution can cause additional loss as the system evolves towards the steady state in the receiving fiber. In the past[2] this loss has been considered part of the total splice loss, but the improvement of fiber quality has reduced this effect significantly for typical lengths between splices. Because we have ignored the power redistribution effects (after the splice), these theoretical results are only strictly valid for short lengths of fiber after the splice; however, they should remain valid for typical distances between splices.

## II. THEORY

The modal amplitude coupling coefficient, $C[m_1\alpha_1; m_2\alpha_2]$, for mode $m_1\alpha_1$ of the transmitting fiber and mode $m_2\alpha_2$ of the receiving fiber is obtained directly from the theory of excitation of weakly guiding fibers.[5] (The variable $m$ is the radial mode number and $\alpha$ is the azimuthal mode number.)

$$C[m_1\alpha_1; m_2\alpha_2] = \frac{1}{2}\left(\frac{\epsilon_{co}}{\mu}\right)^{1/2} \int \bar{E}_{m_1\alpha_1} \cdot \bar{E}^*_{m_2\alpha_2} dA, \tag{1}$$

where for parabolic-index fibers (using the infinite profile approximation) the electromagnetic modal field, $E_{m_1\alpha_1}$, propagating in the $z$ direction in the fiber core is:

$$\bar{E}_{m_1\alpha_1} = \begin{pmatrix} \hat{x} \\ \hat{y} \end{pmatrix} A_{m_1\alpha_1} t^{\frac{|\alpha_1|}{2}} L_{m_1}^{|\alpha_1|}(t) e^{-\frac{t}{2}} e^{-i(\alpha_1\phi+\beta z)}, \tag{2}$$

where $\hat{x}$ and $\hat{y}$ are the linearly polarized unit field vectors of the mode. $\epsilon_{co}$ and $\mu$ are the permittivity and permeability of the core, respectively, and $\epsilon_{co} = n_{co}^2\epsilon$. Then

$$A_{m_1\alpha_1} = \left[\left(\frac{\mu}{\epsilon_{co}}\right)^{1/2} \frac{V}{\pi a^2} \frac{m_1!}{(m_1 + |\alpha_1|)!}\right]^{1/2}, \tag{3}$$

and

$$\left.\begin{aligned} t &= V\left(\frac{r}{a}\right)^2 \\ \beta^2 &= \left(\frac{2\pi}{\lambda} n_{co}\right)^2 - 2N\frac{V}{a^2} \\ V &= \frac{2\pi}{\lambda} n_{co} a\sqrt{2\Delta}, \end{aligned}\right\} \tag{4}$$

where the principal mode number is $N(= 2m + \alpha + 1)$, and $L_m^{\alpha}(t)$ is an associated Laguerre polynomial. The variable $a$ is the fiber core radius and $\Delta = (n_{co} - n_{cl})/n_{co}$ is the normalized maximum refractive index difference. For weakly guiding fibers the polarization property of the incoming mode is preserved by the splice, as can be seen from eq. (1).

In general we can write:

$$C(m_1\alpha_1; m_2\alpha_2) = K \cdot I(m_1\alpha_1; m_2\alpha_2), \tag{5}$$

where

$$K = \left[\frac{m_1!m_2!}{(m_1 + |\alpha_1|)!(m_2 + |\alpha_2|)!}\right]^{1/2}. \tag{6}$$

$I(m_1\alpha_1; m_2\alpha_2)$ is a function that depends on the type of splice mismatch. Table I shows the expressions for $I(m_1\alpha_1;m_2\alpha_2)$ for the two cases of intrinsic parameter $(V)$ mismatch and transverse offset between identical fibers $(r_o)$. The derivation of these equations is given in the appendix.

For the parameter mismatch case, the coupling coefficients are a function of the ratio of the normalized frequencies of the two fibers. The hypergeometric function, ${}_2F_1$, is, in this case, a power series in $y^2$ of order $m_1$. Note that because azimuthal symmetry is preserved in the splice, only modes with the same azimuthal mode number couple. In the identical fiber transverse offset case, the coupling coefficients are simple products of Laguerre-Gaussian polynomials with argument proportional to the normalized offset $(r_o/a)$. In this case all azimuthal modes have finite coupling coefficients, but, for small offsets, coupling is much stronger for nearest neighbor azimuthal modes.

Assuming a random phase relationship between the modes of the transmitting fiber, the total power coupled into mode $m_2\alpha_2$, $P_{m_2\alpha_2}$, is:

$$P_{m_2\alpha_2} = \sum_{m_1,\alpha_1}^{T} |C(m_1\alpha_1; m_2\alpha_2)|^2 P_{m_1\alpha_1}, \tag{7}$$

and the total splice loss, $\delta_s$, is then:

$$\delta_s = -10 \log \left( \frac{\sum\limits_{m_2,\alpha_2}^{R} P_{m_2\alpha_2}}{\sum\limits_{m_1,\alpha_1}^{T} P_{m_1\alpha_1}} \right) \tag{8}$$

The mode mixing factor, $\Gamma$ (i.e., the fraction of the power that is redistributed into different modes), is:

$$\Gamma = 1 - \frac{\sum\limits_{m_1=m_2,\alpha_1=\alpha_2}^{T} |C(m_1\alpha_1; m_2\alpha_2)|^2 P_{m_1\alpha_1}}{\sum\limits_{m_2,\alpha_2}^{R} P_{m_2\alpha_2}}. \tag{9}$$

The superscripts $R$ and $T$ refer to sums over the bound mode spectra of the receiving and transmitting fibers, respectively.

The range of allowed radial and azimuthal mode numbers, $m$ and $\alpha$, for a fiber with normalized frequency $V$ is:

$$\begin{aligned} m \leqslant m_{\max} &= \mathrm{INT}(V/4) \\ \alpha \leqslant \alpha_{\max} &= \mathrm{INT}(V/2) - 1 \\ N_{\max} &= \mathrm{INT}(V/2), \end{aligned} \tag{10}$$

Table I—Mode coupling functions

| Splice | Parameter of Fiber: Transmitting | Parameter of Fiber: Receiving | $I(m_1\alpha_1; m_2\alpha_2)$ |
|---|---|---|---|
| Parameter Mismatch | | | $= 0$ for $\alpha_1 \neq \alpha_2$ |
| | $a_T$ | $a_R$ | $= \dfrac{(m_1+m_2+\alpha)!}{m_1!m_2!} \cdot \dfrac{(1+\epsilon)^{(\alpha+1)/2}}{\left(1+\dfrac{\epsilon}{2}\right)^{\alpha+1}} \cdot (-1)^{m_1}$ |
| | $\Delta_T$ | $\Delta_R$ | $\cdot y^{-(m_1+m_2)}\, {}_2F_1[-m_2;-m_1;-(m_1+m_2+\alpha);y^2],$ |
| | $V_T$ | $V_R$ | where $y = (2+\epsilon)/\epsilon$ and $\epsilon = \left(\dfrac{V_R}{a_R^2} \cdot \dfrac{a_T^2}{V_T}\right) - 1$ |
| Transverse Offset for Identical Fibers | $a$ | $a$ | $= (R_o)^{p/2} e^{-R_o} \cdot \phi(m_1\alpha_1; m_2\alpha_2)$ for $\alpha_1 > 0$, $\alpha_2 < 0$; |
| | $\Delta$ | $\Delta$ | $\phi = L_{m_1}^{\lvert\alpha_2\rvert-\Delta m}(R_o) L_{m_2}^{\lvert\alpha_1\rvert+\Delta m}(R_o)$ for $\alpha_1 > 0$, $\alpha_2 > 0$; |
| | Transverse displacement of the fiber axes $= r_o$ | | $\phi = \dfrac{(m_2+\alpha_2)!}{m_1!} \cdot (-R_o)^{\Delta m} L_{m_2+\alpha_2}^{P+\Delta m}(R_o) \cdot L_{m_2}^{\Delta m}(R_o),$ where $R_o = \dfrac{V}{4}\left(\dfrac{r_o}{a}\right)^2$; $\Delta m = m_1 - m_2$; $p = \lvert\alpha_1 - \alpha_2\rvert$ |

where INT indicates the integer part. It is essential to realize the discrete nature of the bound mode spectra to understand the splice loss predictions for intrinsic parameter ($V$) mismatch. The explicit wavelength dependence of splice loss and mode mixing is demonstrated by the presence of $V$ in the coupling coefficients. However, an implicit wavelength dependence due to the allowed spectrum of bound modes occurs from eq. (10).

## III. RESULTS

Equations (8) and (9) can be used to calculate splice losses and degree of mode mixing for the two cases of parameter mismatch and transverse offset. To validate this analysis, they must be compared with existing theories wherever possible. Most existing results are geometric optics evaluations of splice loss, and the modal power distribution equivalent to any assumed ray distribution is difficult to evaluate in general. However, the ray distribution equivalent to the uniform modal power distribution has been well documented,[6] and comparison of splice loss predictions for this case demonstrates that this analysis is correct. Calculations and experimental results for the effects of different modal power distributions on the mode mixing and loss at a splice are shown in the sections that follow.

### *3.1 Identical fiber transverse offset*

This section presents the results for mode mixing and splice loss associated with transverse offset of the fiber axes for identical fibers.

#### *3.1.1 Splice loss*

Splice loss predictions for transverse offset with a uniform power distribution for several values of the normalized frequency, $V$, are shown in Fig. 1. It is well known that, as $V$ increases, the electromagnetic analysis should asymptotically approach the geometric optics predictions. This is confirmed in Fig. 1. The only other published electromagnetic splice loss theory[3] does not appear to converge to the correct geometric optics limit, e.g., from Fig. 3 of Ref. 3, the splice loss for $0.2a$ offset (for $2a = 50$ $\mu$m) is ~1.0 dB, whereas geometric optics predict a value of 0.8 dB. The small deviation of our results for small offset ($<0.1a$) is believed to be caused by coupling of power to the bound modes of the receiving fiber through the evanescent cladding fields. This effect cannot be predicted using ray optics.

Uniform power distribution results do not agree with realistic splice loss measurements.[2] Figure 2 demonstrates loss versus transverse offset for several power distributions, the Gaussian splice loss model,[2] and experimental data.[8] The experimental data shown were obtained using 0.82-$\mu$m laser excitation of a 7-km input fiber containing about

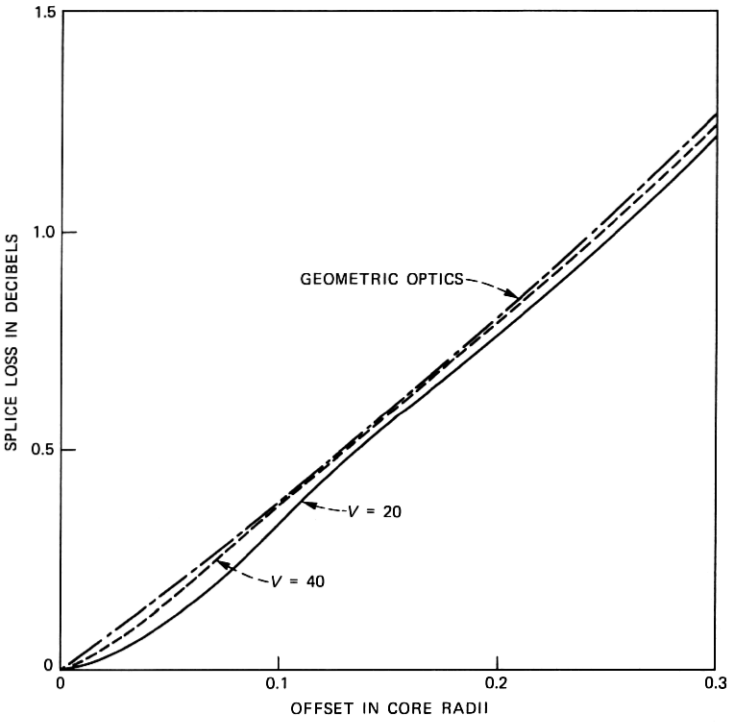


Fig. 1—Splice loss vs. transverse offset with uniform input power.

14 splices into a final splice that was offset in both $x$ and $y$ orthogonal axes. The offset data are in good agreement with previous data and should represent a realistic "steady-state" condition. The theoretical power distribution for steady state due to microbending[4] gives excellent agreement with this data. (A power distribution that has been used to approximate this steady-state distribution is also plotted to show the sensitivity of the loss to the choice of power distribution.) The excellent agreement between the data and this analysis using the steady-state power distribution confirms both the distribution and the splice loss theory. Although this power distribution gives excellent agreement with the data for very long lengths of fiber before the splice, it does not agree as well as the Gaussian model[2] with shorter-length input fiber measurements because the power distribution has not achieved "steady state."

Figure 3 compares experimental data for shorter lengths of input fiber (~1 km) and different excitation conditions[8] with theoretical predictions using both the Gaussian model[2] and various power distributions in this modal analysis. Note that the different excitation conditions significantly affect the splice loss for larger offsets. The

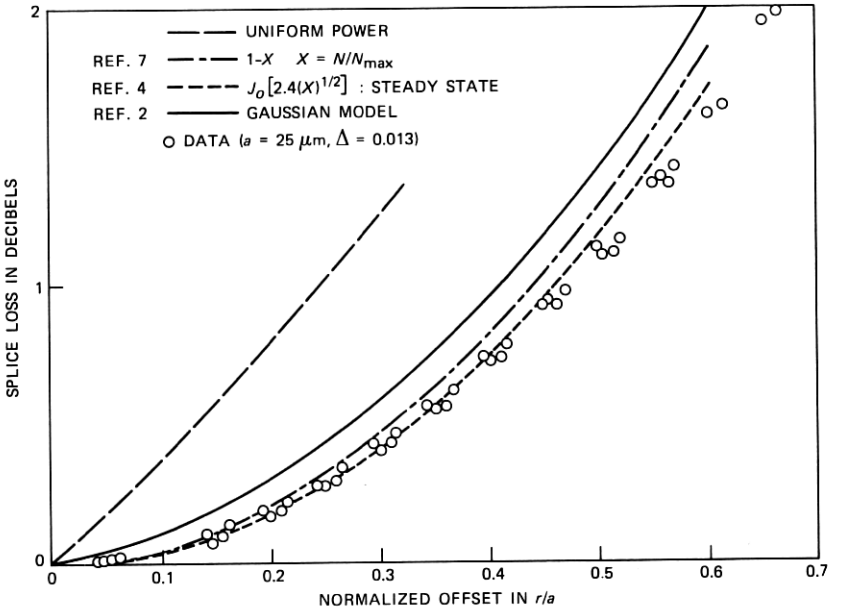


Fig. 2—Loss vs. transverse offset for different modal power distributions.

empirical model of Ref. 2 agrees well with loss measurements for typical offsets expected in practice of 0.1 to 0.2 ($r_o/a$) for both sources and agrees very well over a wider range for the laser source. Modal power distributions for the electromagnetic analysis to describe this situation were empirically chosen so that, for very long fiber lengths, they would degenerate to the steady-state distribution. The simplest choice for a power distribution satisfying this criteria is:

$$P(m_1\alpha_1) = J_o\left[2.405\sqrt{\frac{N}{N_{\max}}}(1 - e^{\eta L})\right]. \tag{11}$$

The choices of $\eta$ shown in Fig. 3 (for $L = 1$ km) demonstrate that excellent agreement between the modal analysis and the splice loss versus transverse offset for the shorter input fiber lengths is possible for both sources. Furthermore, for $\eta = 3$, the results agree with the predictions of the empirical model[2] within 0.03 dB. The theoretically predicted steady-state distribution gives optimistic results for this short length. The existence of a modal power distribution that is in good agreement with the results of Ref. 2 for transverse offset supports the basic assumptions of the empirical model.

### *3.1.2 Mode mixing*

Equation (9) can be used to calculate the amount of power in the

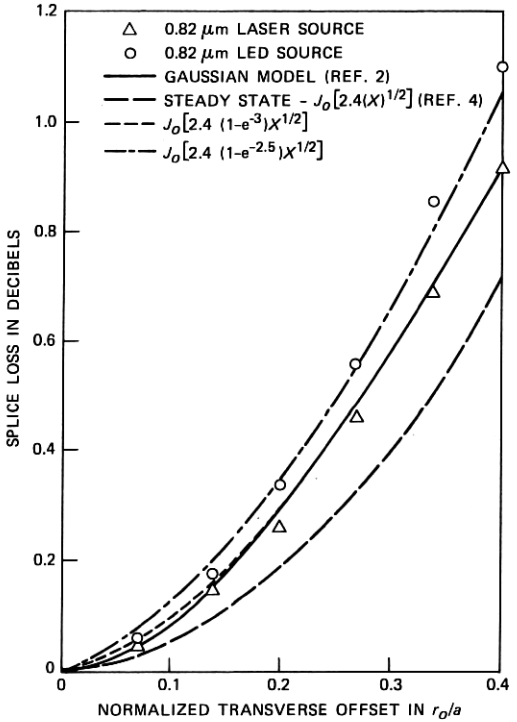


Fig. 3—Splice loss vs. transverse offset for 1-km input fiber.

receiving fiber that has changed propagation mode because of the splice. By changing the summation criteria one can calculate any desired mode mixing factor, such as power coupled within the same principal mode group, nearest neighbor mode groups, etc., where the summation is over all $m_1$, $\alpha_1$ and $m_2$, $\alpha_2$ that differ in principal mode number by $\Delta N$, which is written as:

$$\sum_{2m_2+\alpha_2-2m_1-\alpha_1=\Delta N} \quad \text{for} \quad \Delta N = 0, 1, 2, \cdots . \tag{12}$$

Mode mixing as a function of normalized transverse offset for two different input power distributions is shown in Fig. 4 as the percentage of receiving fiber power that has been redistributed into neighboring mode groups. These differ in principal mode number, $N$, by $\Delta N$ of 0, 1, 2, 3, and 4. ($\Delta N = 0$ represents power coupled within the same degenerate mode group in both transmitting and receiving fibers.) The power distributions used were the uniform and the theoretically predicted power distribution for the steady state for microbending.[4] It is important to note that the percentage of the power-changing propagating mode groups is very high even for small offsets with low splice

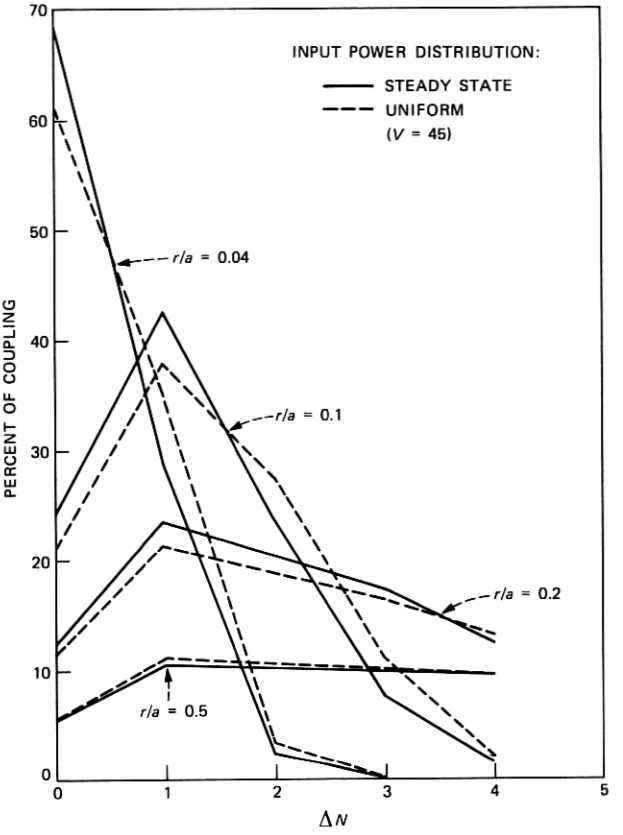


Fig. 4—Power coupling into neighboring mode groups for transverse offset.

loss, i.e., 31 percent for $0.04a$ offset and 0.07 dB splice loss for a $V = 45$ fiber with the steady-state power distribution. Mode mixing is a fairly weak function of the modal power distribution, which indicates that the mode mixing is uniform over all the mode groups as can be seen from the local numerical aperture arguments.[2] As offset increases, the mode mixing changes from being primarily to the nearest neighbor mode groups ($\Delta N = \pm 1$) to being redistributed over a wider range of principal mode groups. The strength of the mode coupling for even small offsets with low splice loss, and the relatively small offsets at which it spreads over many mode groups, are both initially surprising.

### *3.2 Parameter mismatch*

For fibers with no axial offset, the individual mode fields are insensitive to small changes in the $V$ parameter, so that for splices with only slight parameter mismatch, as can be seen in eq. (1), self-coupling

dominates (i.e., mode $m_1\alpha_1$ of the transmitting fiber couples primarily with mode $m_1\alpha_1$ of the receiving fiber). For example, there is less than 3-percent mode mixing for a 5-percent parameter mismatch with uniform modal excitation over the wavelength range of 0.8 to 1.4 $\mu$m. Therefore, splice loss due to parameter mismatch is caused only by this slight field mismatch unless the ranges of the bound mode spectra of the two fibers [eq. (10)] differ, i.e., if the normalized frequencies of the fibers are such that $\Delta N_{\max} \geq 1$. In that case:

$$\Delta N_{\max} = N^T_{\max} - N^R_{\max} \tag{13}$$

or

$$\Delta N_{\max} = \text{INT}\left[\frac{\pi}{\lambda} n_{co}(a_T\sqrt{2\Delta_T})\right] - \text{INT}\left[\frac{\pi}{\lambda} n_{co}(a_r\sqrt{2\Delta_R})\right]. \tag{14}$$

When $\Delta N_{\max}$ is zero, the splice loss is small, as discussed above. However, when $\Delta N_{\max} > 0$, the modes in the highest-order mode group of the transmitting fiber are not bound modes in the receiving fiber. Because self-coupling dominates, most of the power in the highest-order modes couples to leaky/radiation modes in the receiving fiber and is therefore lost. The large degeneracy of the higher-order mode groups [eq. (4)] accentuates this loss. From this discussion we see that parameter mismatch splice loss is caused primarily by the difference between the bound mode volumes of the two fibers, which is a function of the normalized frequencies, $V$. Therefore, both $\Delta$ and radius mismatches can be expressed simply as $V$ mismatch. (An $x$-percent radius mismatch is equivalent to a $2x$-percent $\Delta$ mismatch for small degrees of mismatch.)

Theoretical predictions of splice loss versus normalized parameter mismatch ($\Delta V/V$) for uniform and steay-state input power distributions at 0.82 and 1.3 $\mu$m are shown in Fig. 5. The discontinuities of the splice loss curves are caused by the discreteness of the bound mode spectra, as can be seen from the definition of $\Delta N_{\max}$ in eq. (14). In Fig. 5a this discreteness is most obvious due to the choice of a uniform input power distribution, which accentuates the power in the highest-order mode group. Note that at the longer wavelength the loss is initially higher for a given parameter mismatch because the percentage of the total power that is in the highest-order mode groups is greater than at shorter wavelengths. Each discontinuous increase of splice loss is caused by the stripping of an additional high-order mode group of the input fiber, which does not propagate in the receiving fiber as $\Delta V/V$ increases. The splice loss predicted by geometric optics (which ignores the discreteness of the mode spectra) is also shown.[1] The results for the steady-state power distribution used previously are shown in Fig. 5b displaying similar discontinuous features. However,

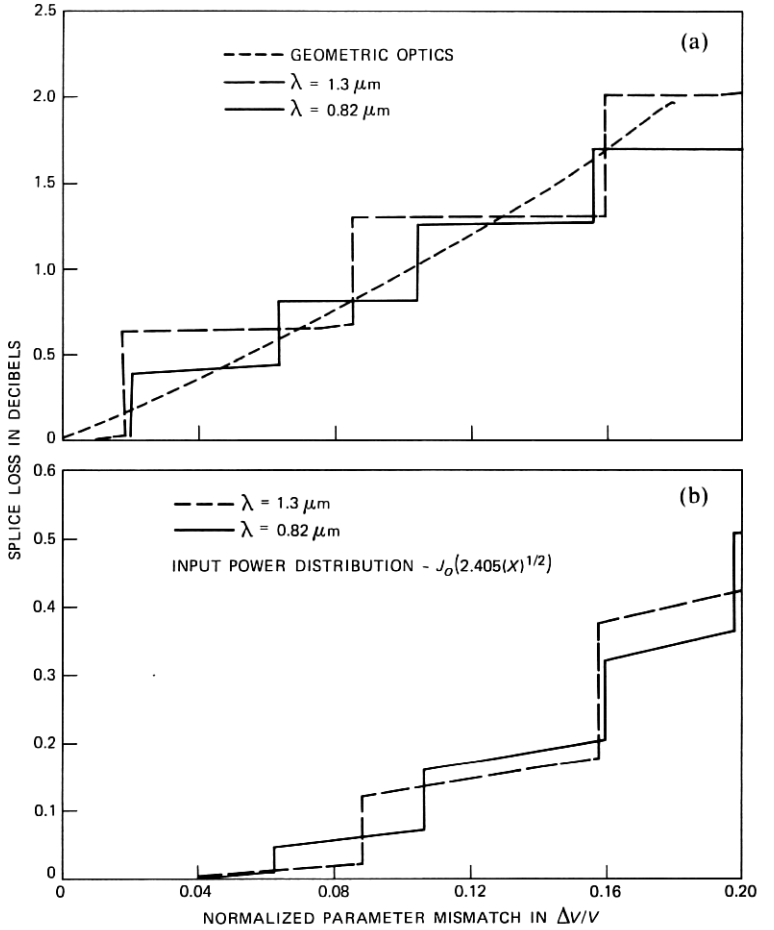


Fig. 5—Splice loss vs. normalized parameter mismatch in $\Delta V/V$ for (a) uniform power distribution and (b) steady-state power distribution.

the decrease in the order of magnitude of the loss allows the observation of the small loss component caused by the slight field mismatch between similar modes of the two fibers. This is reflected in the small slope of the levels. Because the steady-state distribution assumes that there is no power in the highest-order mode group of the transmitting fiber, the first discontinuous change of splice loss of Fig. 5a is negligible in Fig. 5b.

Figure 6 shows the percentage of mode mixing at a splice caused by parameter mismatch for 0.82- and 1.3-μm wavelengths, and the uniform and steady-state power distributions. The substantially higher mode mixing for the uniform power case compared to the steady-state indicates that mode mixing is dominated by the higher-order modes.

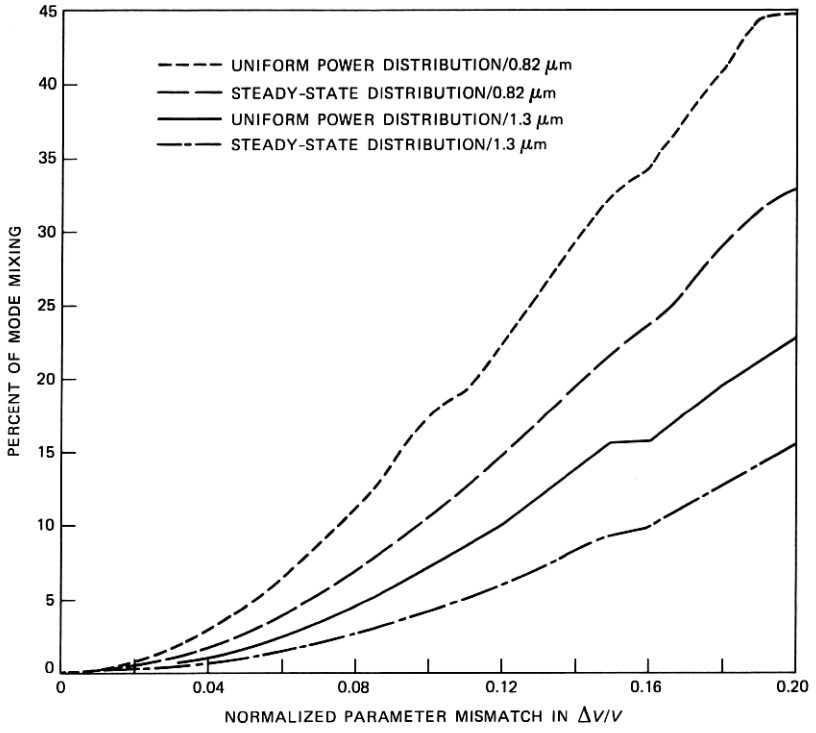


Fig. 6—Percent of mode mixing vs. normalized parameter mismatch.

This contrasts with the transverse offset case shown in Fig. 4, where mode mixing is essentially the same for uniform and steady-state distributions. Reduced mode mixing at longer wavelengths is due to the more diffuse bound mode fields, which result in stronger self coupling between modes. In comparison to the transverse offset case, the degree of mode mixing for the case of parameter mismatch is substantially reduced. Furthermore, a detailed analysis of the mode mixing shows that the coupling is almost completely nearest neighbor coupling ($\Delta N = 1$), e.g., for $\Delta V/V \sim 0.2$, 38 percent of the total 44-percent mode mixed power is coupled to nearest neighbor modes. The deviations from a smoothly increasing function in these curves occur at the transition points of the splice loss curves (see Fig. 5). This is caused by the transition of the highest-order mode group in the receiving fiber from propagating to lossy, removing its contribution to the overall mode mixing.

### *3.3 Wavelength dependence of splice loss for parameter mismatch*

As we can see from eq. (13), for a given degree of parameter mismatch, $\Delta N_{max}$ is also a discontinuous function of wavelength. For

example, if, at some particular wavelength, $V_T$ is 46.1 and $V_R$ is 45.9, $\Delta N_{max}$ is 1 and splice loss is ~0.5 dB. A slight change of wavelength (~1 percent) will cause both $V$'s to simultaneously be greater or less than 46 with $\Delta N_{max} = 0$, and splice loss is ~0.02 dB. Theoretical considerations [eq. (14)] also indicate that the period of the splice loss fluctuations should increase with increasing wavelength because the mode volume is proportional to $1/\lambda$. The magnitude of the fluctuation should also increase with wavelength because the relative amount of power in the highest-order mode group increases as the mode volume decreases. The splice loss wavelength dependence for a parameter mismatch ($\Delta V/V$) of 0.04 and uniform input power distribution is shown in Fig. 7. The magnitude of the splice loss changes considerably over the entire wavelength range. Splice loss calculated from geometric optics for this parameter mismatch case is also shown in Fig. 7 and is approximately the wavelength averaged splice loss as calculated from modal theory. Although the splice loss displays this pathological behavior, the mode mixing remains relatively small and continuous.

Figure 8 gives two further examples of the theoretical splice loss versus wavelength for uniform power excitation and core radius mismatches of 1.0 and 1.5 $\mu$m. For $\Delta a$ of 1.5 $\mu$m, there are ranges of wavelength over which $\Delta N_{max} = 2$, resulting in even larger fluctuations. The choice of a uniform power distribution unrealistically enhances the magnitude of this effect. For example, with the choice of the steady-state distribution, there would be very little power in the highest-order mode group, and therefore this change in loss would be very small, as we can see in Fig. 5b. Splice loss is not expected to vary as abruptly as shown in Figs. 7 and 8, even for a uniform power distribution, because the cladding splits the degeneracy of the highest-order mode group and some modes of this group remain bound even when the group itself, as predicted by the infinite parabolic approxi-

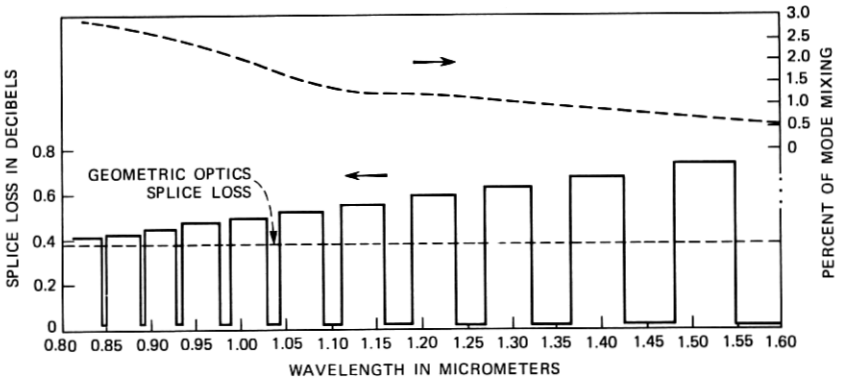


Fig. 7—Splice loss and mode mixing vs. wavelength for $\Delta V/V = 0.04$.

mation, is not bound. This results in a smoothing of the loss versus λ curve, but the periodicity should not be affected. The observation of this effect would further verify this analysis.

### *3.4 Experiment*

The experimental setup shown in Fig. 9 was designed to enhance the power in higher-order mode groups in an attempt to observe the predicted wavelength dependence of splice loss shown in Figs. 7 and 8. A 5 m, 63-μm core, step-index fiber was over-filled and used to excite

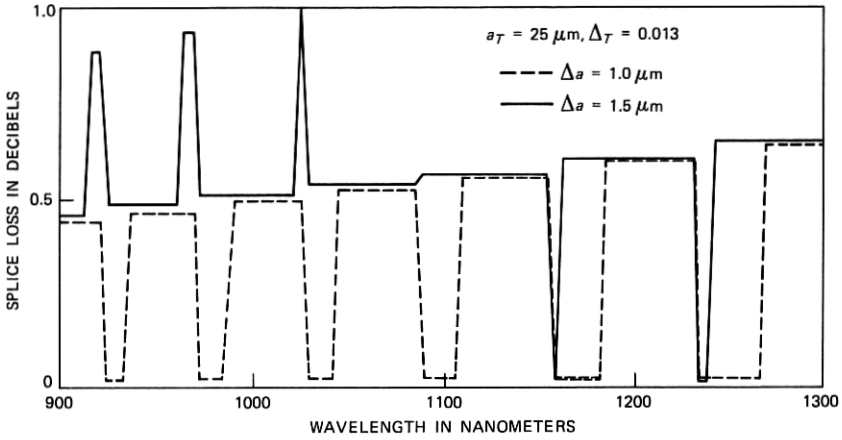


Fig. 8—Theoretical loss vs. wavelength for parameter mismatch.

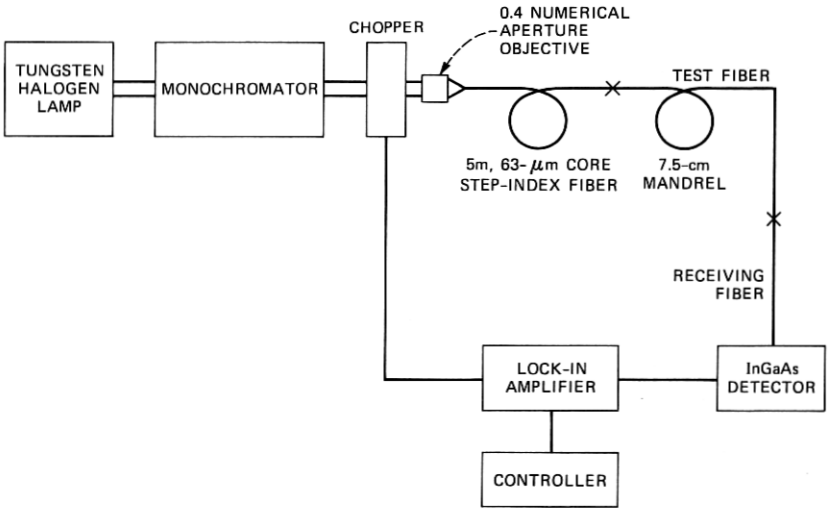


Fig. 9—Splice loss measurement system.

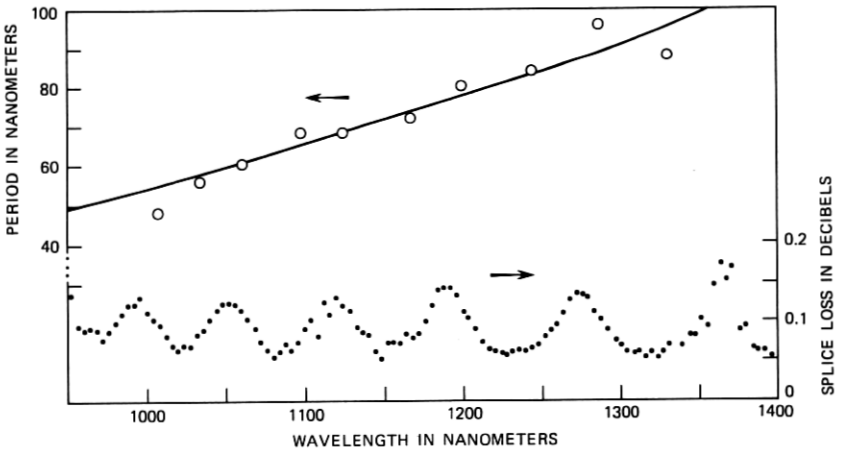


Fig. 10—Measured period and splice loss for parameter mismatch.

the test fiber, which was wound on a 7.5-cm mandrel. A cut-back test determined that approximately 15 m of fiber on this mandrel successfully eliminated leaky modes in the transmitting fiber. This fiber was spliced with micropositioners to a 1 to 2 m length of fiber, which differed in core radius by 1.0 ± 0.2 $\mu$m (but with the same $\Delta$), as determined by refracted near-field measurements. Monochromator resolution was 2 nm and the repeatability of the splice loss measurements was 0.02 dB. As a final check the test fiber was spliced to a length of identical fiber. Maximum splice loss change seen in this case was 0.02 dB, with no discernible wavelength dependence.

The measured wavelength dependence of splice loss and its period are plotted in Fig. 10 for the mismatched fibers. The data show excellent agreement with the period versus wavelength curve obtained from Fig. 8. The increase in maximum amplitude with wavelength seen in Fig. 10 is in qualitative agreement with the theory. Cladding effects (ignored in the infinite parabolic approximation) and only partial success in achieving a uniform power distribution are the probable reasons that the maximum amplitude is less than expected from Fig. 8.

## IV. CONCLUSIONS

In this paper we have presented a modal theory that allows the calculation of mode mixing and loss resulting from parabolic-index multimode fiber splices. The predictions of this model have been confirmed by experiment, including a previously unreported wavelength dependence of splice loss for intrinsic parameter mismatch.

This phenomenon is not expected to be significant for practical "steady-state" system losses but is important for providing insight into the actual loss mechanisms at a splice as well as verifying the validity of the theory. Another effect of this discreteness of the bound mode spectrum has previously been reported for the wavelength dependence of bending loss.[9] The theory also successfully describes splice loss versus transverse offset phenomena and has been used to verify the predicted steady-state power distribution. The analysis provides a basis for understanding mode-mixing effects at splices, which is important for bandwidth studies on concatenated fiber lengths. Splice losses caused by offset or parameter mismatch produce greatly different degrees of intermodal coupling. This implies that the effect of the splice on the bandwidth of a concatenated length is insignificant for the case of small parameter mismatch, but may be significant for transverse offset (due to the strong mode mixing). The sensitivity of the splice loss predictions to the choice of the input power distribution may allow this analysis to provide an evaluation of modal power distributions in fibers from experimental measurements of splice loss versus transverse offset.

The particular case of longitudinal offset has been obtained from a generalization of the parameter mismatch theory but has not been treated here due to its relative unimportance in practical systems. Gloge used geometric optics to show that fiber axis tilt at the splice is equivalent to a transverse offset via the relationship $(r_o/a)^2$ is equal to $\sin^2\theta/2\Delta$, where $\theta$ is the angle between the fiber axes.[10] This equivalence is also valid from the electromagnetic analysis for pure tilt or offset. The modal analysis of combinations of offset (both transverse and longitudinal) with tilt and parameter mismatch (as discussed in Ref. 10) are subjects of continuing work.

## V. ACKNOWLEDGMENTS

We would like to thank D. W. Peckham for providing loss versus transverse offset data; M. J. Saunders for index profile data; and C. M. Miller, P. J. Rich, and R. B. Kummer for helpful discussions.

## REFERENCES

1. S. E. Miller and A. G. Chynoweth, Eds., *Optical Fiber Telecommunications*, New York, NY: Academic Press, 1979, p. 74.
2. C. M. Miller and S. C. Mettler, "A Loss Model for Parabolic Profile Fiber Splices," B.S.T.J., *57*, No. 9 (November 1978), pp. 3167–80.
3. N. Kashima, "Transmission Characteristics of Splices in Graded-Index Multimode Fibers," Appl. Optics, *20*, No. 22 (November 15, 1981), pp. 3859–66.
4. D. Marcuse, "Losses and Impulse Response of a Parabolic Index Fiber With Random Bends," B.S.T.J., *52*, No. 8 (October 1973), pp. 1423–37.
5. A. W. Snyder, "Excitation and Scattering of Modes on a Dielectric or Optical Fiber," IEEE Trans., *MTT*-17 (December 1969), pp. 1138–44.
6. D. Gloge and E. A. J. Marcatili, "Multimode Theory of Graded-Core Fibers," B.S.T.J., *52*, No. 9 (November 1973), pp. 1563–78.

7. R. Olshansky, "Mode Coupling Effects in Graded-Index Optical Fibers," Appl. Optics, *14*, No. 4 (April 1975), pp. 935–45.
8. D. W. Peckham, unpublished work.
9. T. Ohshima et al., "Cutoff Wavelength Measurements of a Multimode Fiber," Proc. of 7th E.C.O.C., Copenhagen, Denmark, 1981, pp. 5-1–5-4.
10. D. Gloge, "Offset and Tilt Loss in Optical Fiber Splices," B.S.T.J., *55*, No. 7 (September 1976), pp. 905–16.
11. S. C. Mettler, "A General Characterization of Splice Loss for Multimode Optical Fibers," B.S.T.J., *58*, No. 10 (December 1979), pp. 2163–82.
11. I. S. Gradshteyn et al., *Tables of Integrals, Series, and Products*, New York, NY: Academic Press, 1980, p. 844, Eqn. 7.414.4.
12. N. N. Lebedev, *Special Functions and Their Applications*, Englewood Cliffs, NJ: Prentice-Hall, 1965, p. 83, Eq. 4.20.3.
13. J. A. Stratton, *Electromagnetic Theory*, New York, NY: McGraw-Hill, 1941, p. 373.
14. A. Erdélyi, Ed., *Higher Transcendental Functions*, The Bateman Manuscript Project, New York, NY: McGraw-Hill, Vol. 2, p. 188.
15. Ref. 11, p. 848, Eqn. 7.422.2.
16. A. Erdélyi, Ed., *Tables of Integral Transforms*, The Bateman Manuscript Project, New York, NY: McGraw-Hill, 1954, Vol. 2, p. 43.

## APPENDIX

### *Derivation of Modal Coupling Coefficients*

The principal steps in the derivation of the modal coupling coefficients (eq. 1) presented in Table I are shown in this appendix.

#### *A.1 Intrinsic parameter (V) mismatch*

In this case both fibers have fields as defined in eq. (2), where the argument of the field, $Z$, is

$$Z_T = V_T(r/a_T)^2 \tag{15}$$

and

$$Z_R = Z_T(1 + \epsilon), \tag{16}$$

where

$$V_T = (2\pi/\lambda) \cdot n_{co} \cdot \sqrt{2\Delta_T} \cdot a_T \tag{17}$$

and

$$\epsilon = \left(\frac{V_R}{a_R^2}\right)\left(\frac{a_T^2}{V_T}\right) - 1, \tag{18}$$

where the normalization expressions $A_{m\alpha}$ also contain $V_T$ and $V_R$.

Examination of the azimuthal integral of eq. (1) shows that, because there is no transverse offset of the fiber axes, azimuthal symmetry is preserved and only modes with the same azimuthal symmetry couple.

Changing the radial integral from an integration over $r$ to one over $Z_T$, we find that it is in the form of a well-documented integral of Laguerre Gaussian functions,[11] giving the expression shown in Table I. The hypergeometric function, ${}_2F_1(-m_2, -m_1, -(m_1 + m_2 + \alpha), y^2)$ is a finite power series in $y^2$ whose order is the lesser of $m_1$ or $m_2$, since both $m_1$ and $m_2$ are integers.

### A.2 Transverse offset—identical fibers

The modal fields to be used in eq. (1) can still be expressed by eq. (2) for both fibers. However, the radial and azimuthal variations of the receiving fiber ($r_R$, $\phi_R$) need to be expressed in terms of the transmitting fiber ($r_T$, $\phi$) and the transverse offset, $r_o$, of the axes. Using

$$r_R^2 = r_T^2 + r_o^2 - 2r_T r_o \cos\phi \tag{19}$$

and the integral relation for Laguerre-Gaussian functions[12]

$$e^{-Z/2}Z^{|\alpha|/2}L_m^{|\alpha|}(Z) = \frac{(-1)^m}{2}\int_o^\infty J_\alpha(\sqrt{xZ})e^{-x/2}x^{|\alpha|/2}L_m^{|\alpha|}(x)dx \tag{20}$$

we can then use the addition theorem for circular cylindrical waves[13] to write the receiving fiber field amplitude $E_R(m, \alpha)$ as

$$E_R(m, \alpha) = \frac{(-1)^m}{2}\sum_{p=-\infty}^{\infty} e^{-i(p+\alpha)\phi} \cdot \int_o^\infty J_p(\sqrt{xZ_o})J_{p+\alpha}(\sqrt{xZ_T})e^{-x/2}x^{|\alpha|/2}L_m^{|\alpha|}(x)dx, \tag{21}$$

where

$$Z_o = V(r_o/a)^2$$

$$Z_T = V(r_T/a)^2. \tag{22}$$

The azimuthal integral of eq. (1), for coupling between mode ($m_1\alpha_1$) of the transmitting fiber and mode ($m_2\alpha_2$) of the receiving fiber, reduces the infinite summation over $p$, introduced by eq. (21), to a single term for

$$p + \alpha_2 = \alpha_1. \tag{23}$$

After a change of variable from $r_T$ to $Z_T$ defined above, the radial integral of eq. (1) can be evaluated by again using eq. (20). (In evaluating this integral it is imperative to realize that the radial field variation of the modes is a function only of the magnitude of the azimuthal mode number, $|\alpha|$.) This evaluation produces two cases, which must be treated separately:

(*i*) $\alpha_1$ and $\alpha_2$—both the same sign

(*ii*) $\alpha_1$ and $\alpha_2$—different sign.

For both cases the final integral over the dummy variable $x$, introduced by the Laguerre-Gaussian integral identity [eq. (20)], can be evaluated by using the relationship[14]

$$L_n^{-\delta}(x) = (-1)^\delta x^\delta \frac{(n-\delta)!}{n!}L_{n-\delta}^{\delta}(x) \tag{24}$$

to write the integral in the form

$$I = \int_o^\infty y^{p+1} e^{-\alpha y^2} L_m^{p-\sigma}(\alpha y^2) L_n^{\sigma}(\alpha y^2) J_p(x \cdot y) dy, \tag{25}$$

which is a well-documented integral giving

$$I = (-1)^{m+n}(2\alpha)^{-(p+1)} x^p e^{-x^2/4\alpha} L_m^{\sigma-m+n}(x^2/4\alpha) \cdot L_n^{p-\sigma+m-n}(x^2/4\alpha). \tag{26}$$

In both Refs. 15 and 16, the formula is slightly incorrect due to a reversal of the subscripts of the Laguerre polynomials. The formula of Refs. 15 and 16 is seen to be incorrect by noting that eq. (25) above is a Hankel transform of order $p$, so that, by applying the inverse transform to the result, one should expect to obtain the original function, i.e., the argument of the original Hankel transform. The error persists in Ref. 15 because it used Ref. 16 as its source for this result. The use of this relationship then provides the results in Table I.